PROTEINS: Structure, Function, and Bioinformatics 57:635–638 (2004)

STRUCTURE NOTE

Crystal Structure of the ATP-Binding Cassette of Multisugar Transporter from *Pyrococcus horikoshii* OT3

Toyoyuki Ose, Takeyuki Fujie, Min Yao, Nobuhisa Watanabe, and Isao Tanaka*
Division of Biological Sciences, Graduate School of Science, Hokkaido University, Sapporo, Japan

Adenosine triphosphate (ATP)-binding cassette transporters (ABC transporters), which are ubiquitous in all organisms from bacteria to humans, are ATP hydrolysis-dependent transmembrane transporters or channels.[1] The crystal structure of the ATP-binding subunit (PH0022) of the multisugar transporter, which is the ATPase subunit of the trehalose/maltose transporter ($MalEFGK_2$) homologue from the hyperthermophilic archaebacterium *Pyrococcus horikoshii* OT3, was determined at 2.2 Å. We also report in this article the crystal structure of PH0022 complexed with ATP by a cocrystallization method. Data collection and refinement statistics are summarized in Table I.

The final native model includes 1 protein molecule (residues 1–373) and 99 water molecules. The Matthews' coefficient (V_M) for PH0022 is 2.50 $Å^3$/Da, and the estimated solvent content is 50.3%. The Ramachandran plot produced by PROCHECK[2] shows that 90.0% of the residues are in the most favored region, 9.3% are in additional allowed regions, and 0.7% are in generously allowed regions. The ABC signature region (residues 143–147) cannot be built because of the poor electron density map.

The protomer of PH0022 can be divided into two, N-terminal (residues 1–223) and C-terminal (residues 227–373) domains (Fig. 1). These two domains are connected by a short linker region. The N-terminal residues form an α/β-type ATPase domain [named a nucleotide-binding domain (NBD)], as generally observed in the ABC transporter family. In the NBD, there are further two subdomains: a RecA-like subdomain and an α-helical subdomain (112–160 residues) that is inserted into the RecA-like domain. The α-helical subdomain is specific to ABC proteins, possessing the ABC family signature motif "LSGGQ" from residues 143 to 147.[3] In the C-terminal domain (regulatory domain, RD), 11 strands form a β-barrel surrounded by 4 helices. The RD is not conserved in the bacterial ABC transporters. A structural similarity search performed using the Secondary Structure Matching server (Protein structure comparison service SSM at European Bioinformatics Institute (http://www.ebi.ac.uk/msd-srv/ssm)), indicated that PH0022 is structurally similar to MalK from *Termococcus litoralis* (T.l.MalK)[4] and *Escherichia coli* (E.c.MalK).[5] The amino acid sequence similarity of NBD among these three open reading frames (ORFs) is about 47% identity and that of RD is 11%, whereas the 33% amino acid residues are conserved among these 3 whole ORFs. Therefore, the RD is characteristic to each ATP-binding subunit. In the RD, the identity of amino acid sequences between PH0022 and T.l.MalK is 33% and that between PH0022 and E.c.MalK is 17%, though the same interactions between the two RDs are observed only in the crystal structures of PH0022 and E.c.MalK.

Two protomers in the crystal form a dimeric structure related by a twofold crystallographic axis in both free and ATP-bound structures. The dimeric molecule is Y-shaped; the extensive chamber is in the middle between the twofold-related NBDs. The RD contributes to protomer–protomer interactions and stabilizes the dimer [Fig. 1(b)]. One of the main aims in the structural study of ABC transporters is to understand the power stroke to transport the substrates concomitant with ATP hydrolysis. Therefore, it is important to understand the interactions between subunits. To date, several ATP-binding subunit structures of various ABC transporters have been determined. However, the dimer (or other oligomer) assemblies are so diverse that there is no consistent paradigm of oligomeric interactions from the crystal structures. The intact crystal structures of MsbA[6] and BtuCD[7] from *E. coli* have been reported, and many intersubunit interactions have been observed. It has been suggested that the ATP-binding subunit should play a role in inducing the conformational changes. Among the ATP-binding subunits whose structures have been solved, only T.l.Malk, E.c.Malk, and the glucose transporter GlcV from *Sulfolobus solfatarixus*[8] have been found to have RDs. The important role of the RD of the ABC transporter is supported by the result of many experiments. For example, the RD has been reported to interact with MalT (a specific gene activator of mal gene expression),[9] and the pivot role has been described in the

Grant sponsor: National Project on Protein Structural and Functional Analyses from the Ministry of Education, Science, Sports, and Culture of Japan.

*Correspondence to: Isao Tanaka, Division of Biological Sciences, Graduate School of Science, Hokkaido University, Sapporo 060-0810, Japan. E-mail: tanaka@castor.sci.hokudai.ac.jp

Received 9 March 2004; Accepted 27 March 2004

Published online 22 July 2004 in Wiley InterScience (www.interscience.wiley.com). DOI: 10.1002/prot.20206

TABLE I. Data Statistics

PDB ID	Native 1V43	ATP-complex 1VCI
Data collection		
Wavelength (Å)	1.000	1.000
Resolution range (Å)	60–2.20 (2.24–2.20)	38–2.80 (2.90–2.80)
Space group	$P4_32_12$	$P4_32_12$
Unit-cell parameters (Å)	$a = b = 79.91$, $c = 130.57$	$a = b = 79.84$, $c = 130.08$
No. of observations	142,683 (25,757)	149,406 (15,172)
No. of unique reflections	29,182 (4202)	20,190 (2023)
Completeness (%)	99.5 (99.7)	100 (100)
Multiplicity	4.9 (6.1)	7.4 (7.5)
Averaged I/σ(I)	19.0 (2.2)	18.7
R^a_{merge}	0.025 (0.252)	0.102 (0.387)
Refinement		
Protein atoms	2797	2797
Water atoms	99	87
ATP atoms	0	31
Resolution range (Å)	20–2.2	10–2.9
R^b_{conv}	0.2354	0.2108
R^c_{free}	0.2976	0.2927
RMSD		
Bond lengths (Å)	0.0084	0.0067
Bond angles (°)	1.40	1.25

Values in the parentheses are for the highest resolution shell.
[a]$R_{merge} = \Sigma_h\Sigma_j \mid \langle I\rangle_h - I_{h,j} \mid / \Sigma_h\Sigma_j I_{h,j}$, where $\langle I\rangle_h$ is the mean intensities of symmetry-equivalent reflections.
[b]$R_{conv} = \Sigma_h \| F_o \mid - \mid F_c \| / \Sigma_h \mid F_o \mid$, where F_o and F_c are the observed and calculated structure factor amplitudes, respectively, for the reflection *h*.
[c]R_{free} is equivalent to R_{conv} for an 8% test set of reflections, as the same indexes as the native data, not used in the refinement.

structure of ATP-bound E.c.Malk.[5] However, other interactions have been observed in the several crystal structures of ATP-binding subunits having RD in their C-terminus. Of these, the tertiary structure, as well as the quaternary structure of PH0022, is similar to that of E.c.Malk, especially to open form.[5] The Cα-superposition of PH0022 and E.c.Malk based on RDs [Fig. 1(c and d)] shows that both RDs are imposed well, though the amino acid sequence of the region is generally not conserved.

The conformational changes upon ATP binding have been reported in the structure analysis of the ATP-bound form of E.c.Malk.[5] Compared with E.c.Malk, little movement was observed upon ATP-binding to PH0022. The σA-weighted F_o-F_c map (contoured at 2.1σ) calculated using refined structure clearly shows an ATP molecule around the Waker A motif (from Gly46 to Thr52) (Fig. 2). The adenine base and the ribose are stabilized by van der Waals interactions with Phe22 and Phe25. The corresponding residues in E.c.Malk are Trp13 and Val16. The residues on the Walker A motif interact with the α, β, and γ phosphate groups of ATP. The carbonyl-oxygen atom of Pro51, the amide-nitrogen atoms from Ser46 to Gly50, the side-chain nitrogen of Lys51, and side-chain oxygen of Thr52 are within the hydrogen bond—or the salt bridge—distance (<3.1 Å).

The structures of PH0022 in the absence/presence of ATP should provide valuable insight into dimeric architecture, which has been reported variously in several ABC cassettes and may represent the one snapshot of an intact ABC transporter.

Methods. The PH0022 gene was amplified by the polymerase chain reaction (PCR) method using oligonucleotide primers, 5′-G GTG GTG CAT ATG GGG AAT AAC ATT GAG G-3′ (underlining indicates the upper primer containing the *Nde*I site) and 5′-GG AAG AAA AGG GAA TTC CTA GAC TAT CGC CTT CTC AGC-3′ (underlining indicates the lower primer containing the *EcoR*I site). The PCR products were ligated into the pGEM-T Easy vector (Promega), and the nucleotide sequences were confirmed by DNA sequencing using the Applied Biosystems dRhodamine kit. The PH0022 genes digested by *Nde*I and *EcoR*I from pGEM-T Easy vector were introduced into pET-22b(+) vector (Novagen). After transformation in *E. coli* cells BL21(DE3) (Stratagene), the cells were grown at

Fig. 1. Crystal structure of PH0022. (**a**) Ribbon diagram of *Pyrococcus horikoshii* PH0022 protomer structure color-coded as Rec-A-like subdomain (blue), α-helical subdomain (yellow), and RD (magenta). (**b**) Dimer structure of ATP-bound form. The ATP is shown in a ball-and-stick model, and the atoms are colored as follows: oxygen (red), nitrogen (blue), carbon (yellow), and phosphorus (magenta). (**c**) Top view of the superposition of the Cα-trace between PH0022 and E.c.MalK. The NBD and RD of PH0022 are colored yellow and red, respectively; the NBD and RD of E.c.MalK are colored light-blue and dark-blue, respectively. (**d**) Front view of the superposition of the Cα-trace between PH0022 and E.c.MalK. Each domain is colored the same as (c).

Fig. 2. Stereo view of the electron density (2.1σ contour level) at the active site of NBD of one of the AB homodimers from the F_o-F_c map. The refined ATP molecule (shown in a magenta ball-and-stick model) was omitted in the structure factor calculation. The residues that interact with the α, β, and γ phosphate groups of ATP are also shown in a gray ball-and-stick model. The atoms are colored as follows: oxygen (red), nitrogen (blue), carbon (yellow), sulfate (green), and phosphorus (magenta).

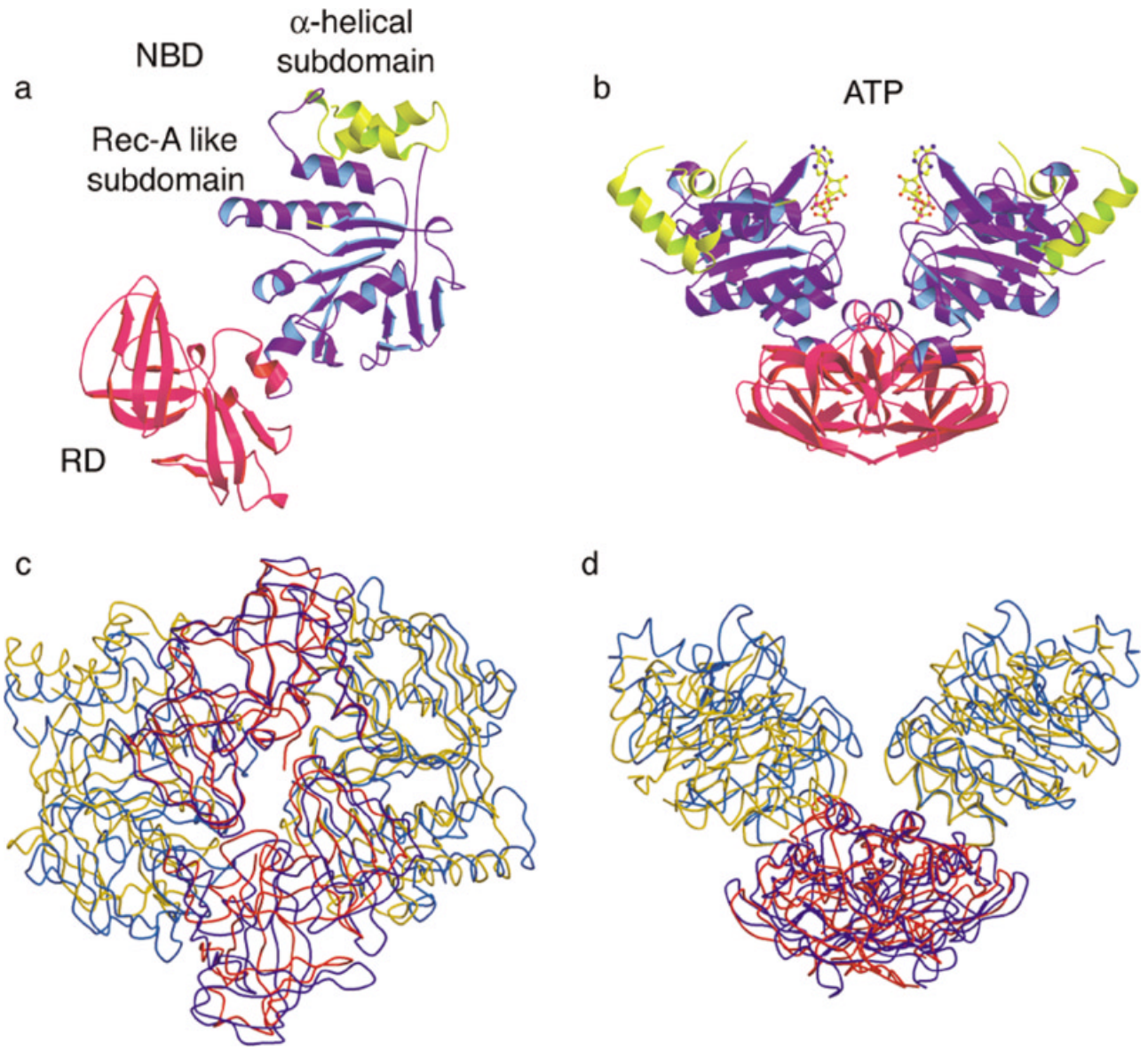

Figure 1.

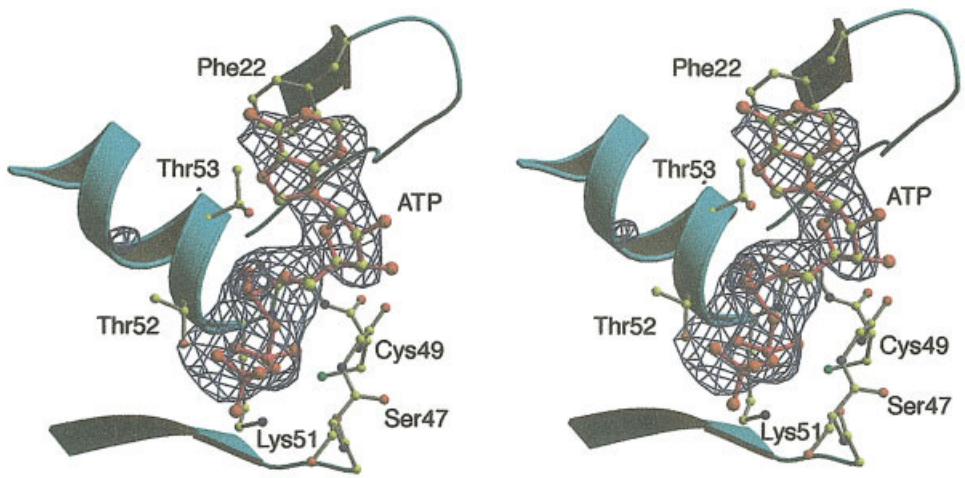

Figure 2.

310 K in Luria–Bertani (LB) medium containing 50 μg/mL^{-1} ampicillin until the optical density (OD) value at 600 nm reached 0.8–1.0.

Overexpression of the recombinant PH0022 was induced by 1 m*M* isopropylthio-D-galactoside (IPTG). After IPTG injection, the cells were grown for 7 h with constant shaking, and harvested by centrifugation at 4000 rpm for 15 min. The cells were then suspended in buffer A (20 m*M* Tris-HCl, pH 7.5) and homogenized by French press (Amico, Inc.) twice at 1000 psi. After centrifugation at 40,000 rpm for 1 h, the supernatant was incubated at 353 K for 30 min and centrifuged at 20,000 rpm for 30 min. The supernatant was dialyzed into buffer B (20 m*M* Tris-HCl pH 7.5, 1.7 *M* ammonium sulfate) and applied to a hydrohobic-interaction Butyl-FF (Amersham Biotech) column equilibrated with buffer B. After washing with buffer B, the bound protein was eluted using a linear gradient of 0–100% buffer A. The fractions containing PH0022 were then applied to HiLoad 20/60 Superdex-200 column (Amersham Biotech) equilibrated with buffer C (20 m*M* Tris-HCl, pH 7.5; 200 m*M* NaCl). The PH0022 was collected as a single peak.

After purification, native PH0022 was dialyzed overnight at 277 K in distilled water and concentrated to 5 mg mL^{-1} using Amicon Ultra (Millipore). Crystals were grown under the conditions of 0.1 *M* Na acetate pH 4.0, 25% w/v ethylene glycol using the hanging-drop vapor diffusion method by mixing 2.5 μL of protein sample with 2.5 μL of reservoir solution. Crystals grew up to 0.4 × 0.4 × 0.1 mm in a week at 291 K. The crystal of ATP-complex PH0022 was prepared by cocrystallization under the conditions of 20mg/mL ATP, 0.1 *M* Na acetate, pH 4.2, 22% w/v ethylene glycol after being heated up to 343 K in 20 min.

Native and ATP-complex data sets were collected at beamline BL41XU of SPring-8 using MAR charge-coupled device (CCD) detector at 1.000 Å wavelength with a flash-frozen technique at 100 K.

The structure of native phMalK was determined by the molecular replacement method using AmoRe.[10] The T. I. MalK structure was used as a search model. Both models of phMalK and phMalK-ATP complex were refined using the program Crystallography & NMR System (CNS) 1.1,[11] and 8% of the reflection data were set aside for the calculation of the free *R*-factor to monitor the refinement. The structure refinement statistics are also shown in Table I. Atomic coordinates have been deposited in the Protein Data Bank (PDB) with PDB-ID 1V43 (native) and 1VCI (ATP-complex).

Acknowledgments. We thank H. Sakai and M. Kawamoto of the Japan Synchrotron Radiation Research Institute (JASRI) for their kind help in data collection on beamline BL41XU at SPring-8.

REFERENCES

1. Higgins CF. ABC transporters: from microorganisms to man. Annu Rev Cell Biol 1993;8:67–113.
2. Laskowski RA, MacArthur MW, Moss DS, Thornton JM. PROCHECK: a program to check the stereochemical quality of protein structures. J Appl Crystallogr 1993;26:283–291.
3. Story RM, Weber IT, Steitz TA. The structure of the *E. coli* recA protein monomer and polymer. Nature 1992;355:318–325.
4. Diederichs K, Diez J, Greller G, Muller C, Breed J, Schnell C, Vonrhein C, Boos W, Welte W. Crystal structure of MalK, the ATPase subunit of the trehalose/maltose ABC transporter of the archaeon *Thermococcus litoralis*. EMBO J 2000;19:5951–5961.
5. Chen J, Lu G, Lin J, Davidson AL, Quiocho FA. A tweezers-like motion of the ATP-binding cassette dimer in an ABC transport cycle. Mol Cell 2003;12:651–661.
6. Chang G, Roth CB. Structure of MsbA from *E. coli*: a homolog of the multidrug resistance ATP binding cassette (ABC) transporters. Science 2001;293:1793–1800.
7. Locher KP, Lee AT, Rees DC. The *E. coli* BtuCD structure: a framework for ABC transporter architecture and mechanism. Science 2002;296:1091–1098.
8. Verdon G, Albers SV, Dijkstra BW, Driessen AJ, Thunnissen AM. Crystal structures of the ATPase subunit of the glucose ABC transporter from *Sulfolobus solfataricus*: nucleotide-free and nucleotide-bound conformations. J Mol Biol 2003;330:343–358.
9. Boos W, Shuman H. Maltose/maltodextrin system of *Escherichia coli*: transport, metabolism, and regulation. Microbiol Mol Biol Rev 1998;62:204–229.
10. Navaza J. AMoRe: an automated package for molecular replacement. Acta Crystallogr A 1994;50:157–163.
11. Brünger AT, Adams PD, Clore GM, DeLano WL, Gros P, Grosse-Kunstleve RW, Jiang JS, Kuszewski J, Nilges M, Pannu NS, Read RJ, Rice LM, Simonson T, Warren GL. Crystallography & NMR System: a new software suite for macromolecular structure determination. Acta Crystallogr D Biol Crystallogr 1998;54:905–921.